International Journal of Pharmaceutics 362 (2008) 133–140

Contents lists available at ScienceDirect

International Journal of Pharmaceutics

journal homepage: www.elsevier.com/locate/ijpharm

Pharmaceutical nanotechnology

Development and evaluation of novel itraconazole-loaded intravenous nanoparticles

Wei Chen [a], Bing Gu [a], Hao Wang [b], Jun Pan [a], Weiyue Lu [a,*], Huimin Hou [b,**]

[a] School of Pharmacy, Fudan University, 138 Yixueyuan Road, Shanghai 200032, China
[b] National Pharmaceutical Engineering Research Center, Shanghai Institute of Industrial Pharmaceutics, 1111 Halei Road, Shanghai 201203, China

ARTICLE INFO

Article history:
Received 19 February 2008
Received in revised form 29 May 2008
Accepted 31 May 2008
Available online 7 June 2008

Keywords:
Itraconazole
Nanoparticle albumin bound technology
Pharmacokinetics
Tissue distribution

ABSTRACT

The purpose of this study was to present novel intravenous itraconazole-loaded nanoparticles (ITZ-NPs) using human serum albumin (HSA) as drug carrier materials. The ITZ-NPs were prepared by nanoparticle albumin bound technology involving a series of homogenization and lyophilization procedures. The ITZ-NPs powder could be easily reconstituted and provide stable solutions at a wide range of concentrations at 25 °C for 24 h. In safety test, the ITZ-NPs caused mild hemolysis below the concentration of 10 mg/mL and were well tolerated at the dose of 160 mg/kg in mice, indicating better biocompatibility than cyclodextrin formulation of itraconazole (ITZ-CD). The pharmacokinetic parameters of itraconazole and its major metabolite, hydroxyl-itraconazole, of ITZ-NPs had no differences from those of ITZ-CD in mice. For the ITZ-NPs group, the distributions of itraconazole in the lung, liver and spleen were higher than those for ITZ-CD group. It was of significance that ITZ-NPs increased the drug distribution in lung which was always the portal to fungal infection. These results indicate that the ITZ-NPs can be a potential intravenous formulation of itraconazole.

1. Introduction

Itraconazole, an azole antifungal agent, is widely clinically used for a variety of serious fungal infections in normal and immunocompromised hosts, including *Aspergillosis*, *Cryptococcus*, *Candida*, *Blastomyces*, disseminated *Penicillium mameffei* infections and *Histoplasma capsulatum var. capsulatum* (Grant and Clissold, 1989; Lortholary et al., 1999). It acts by impairing the synthesis of ergosterol, essential component of the fungal cell membrane (Van Cauteren et al., 1987). The antifungal activity of its major metabolite, hydroxyl-itraconazole (OH-itraconazole), is usually assumed to be equivalent to that of itraconazole (Mikami et al., 1994; Odds and Bossche, 2000). Compared with other conventional antifungal agent, itraconazole has less nephrotoxicity than amphotericin B (Cohen, 1998; Walsh et al., 2004) and broader spectrum of activity than fluconazole, etc. (Revankar et al., 1996). Itraconazole has been orally administered to treat *Candida infections* (Edwards et al., 1997; Phillips et al., 1998). However, intravenous formulation of itraconazole is badly needed for many neutropenic and other immunocompromised patients who have difficulty swallowing the oral capsule formulation (Edwards et al., 1997; Sheehan et al., 1999; Groll et al., 2002). On the other hand, intravenous formulation can reach high plasma concentration quickly, which is vital for itraconazole as there is a well-defined quantitative correlation between its *in vitro* MIC activity and clinical performance in the treatment of *Candidiasis* (Rex et al., 1997).

However, itraconazole is insoluble in aqueous media ($S \sim 1$ ng/mL at neutral pH and $S = 4$ μg/mL at pH 1), the calculated log P is 6.2 (Peeters et al., 2002). It is a tough problem to develop intravenous formulation for insoluble drugs like itraconazole. SPORANOX I.V. is the only commercial available intravenous formulation of itraconazole solubilized by hydroxypropyl-β-cyclodextin (HP-β-CD), which facilitates the establishment of high and dependable levels of the compound in plasma. It has been successfully used in the treatment of severe necrotizing pneumonias, invasive pulmonary *aspergillosis* and so on (Picardi et al., 2003; Groll et al., 2002). Nevertheless, SPORANOX is forbidden to be used in patients with impaired renal function. It is not because of the toxicity of the drug itself, but the adjuvant HP-β-CD. Each milliliter of SPORANOX contains 10 mg of itraconazole solubilized by 400 mg of HP-β-CD as an inclusion complex. Following a single intravenous dose of 200 mg SPORANOX to the subjects with severe renal impairment, clearance of HP-β-CD was six-fold reduced compared with subjects with normal renal function. Although its clinical relevance is unknown, it has been reported

* Corresponding author. Tel.: +86 21 54237143; fax: +86 21 64178790.
** Corresponding author. Tel.: +86 21 51320211.
E-mail address: wylu@shmu.edu.cn (W. Lu).

0378-5173/$ – see front matter © 2008 Published by Elsevier B.V.
doi:10.1016/j.ijpharm.2008.05.039

that HP-β-CD produced pancreatic adenocarcinoma in rat carcinogenicity study (Thomson and Montvale, 2005). Hence, an intravenous formulation of itraconazole without HP-β-CD is of great potential.

Nanoparticle albumin bound technology was an original technology for water-insoluble pharmaceutical active agents (Desai et al., 1999) based on the principle that a large number of water-insoluble drugs have high plasma protein-binding ratio. For example, the plasma protein-binding ratio of itraconazole is 99.8% (Heykants et al., 1987). The key point of the technology thereby was to "pre-bound" the pharmacologically active agents to protein prior to administration. The craft of this technology was as following described. Firstly, the drug was dissolved in a water-insoluble organic solvent and emulsified in water under high-pressure homogenization using protein as the stabilizing agent, which could bind with drugs and lower the interfacial energy between oil and water. Secondly, the organic solvent was removed so that the drug precipitated and protein coated nanoparticles formed immediately. Finally, the nanoparticle powder was obtained through lyophilization. Human serum albumin (HSA) was an excellent carrier in nanoparticle albumin bound technology for its endogenous, non-toxic and non-immunogenic properties. Because no other conventional surfactants or polymeric materials were utilized in the procedure, the albumin nanoparticles would produce less allergic or toxic effects.

In our study, itraconazole-loaded nanoparticles (ITZ-NPs) were developed by nanoparticle albumin bound technology using HSA as stabilizing agent. The physicochemical characterization, *in vitro* release behavior, stability and hemolysis property of the ITZ-NPs were evaluated. Meanwhile, acute toxicity, pharmacokinetics and tissue distribution of the ITZ-NPs, were investigated in mice in comparison with the cyclodextrin formulations of itraconazole (ITZ-CD).

2. Materials and methods

2.1. Materials, reagents and animals

Itraconazole was purchased from Tianjin LiSheng pharmaceutical Co. Ltd., China. HSA (>98%) was purchased from Sigma, USA. The cyclodextrin formulation of itraconazole (ITZ-CD: Sporanox® Injection) was purchased from Janssen Pharmaceutica of Belgium. Hydroxyl-itraconazole (OH-itraconazole) and the internal standard (R051012) were kindly supplied by Janssen Research Foundation (Belgium). All other chemicals were of HPLC or reagent grade and used without further purification.

The animals used in the experiments were supplied by the Department of Laboratory Animal Science, Fudan University, treated according to the protocols evaluated and approved by the Ethical Committee of the University.

2.2. Preparation of ITZ-NPs

ITZ-NPs were prepared using nanoparticle albumin bound technology (Desai et al., 1999). Briefly, 2000 mg HSA was dissolved in 100 mL of water saturated with chloroform. 262.5 mg itraconazole was dissolved in 5.25 mL of chloroform saturated with water. The HSA solution was mixed with itraconazole solution and the mixture was homogenized (EmulsiFlex-C5 homogenizer, Canada) under 20,000 psi for nine cycles. The resulting colloids suspension was rotary evaporated to remove chloroform at 25 °C for 15 min under reduced pressure. Then the nanoparticles were filtered through a 0.22-μm microporous membrane filter and the solvent was removed through lyophilization for 48 h at −70 °C without adding any cryoprotectant (Martin Christ, Germany). The obtained ITZ-NPs powder was vacuum-dried for 24 h and stored under 4 °C, which could be easily reconstituted in normal saline by mild shaking before application. The NPs colloids solution was light blue in color with opalescence.

2.3. Characterization of ITZ-NPs

2.3.1. Particle size and zeta potential measurement

The mean particle size of the ITZ-NPs was measured via dynamic light scattering method (NicompTM 380ZLS zeta potential/particle sizer, Santa Barbara, USA). The ITZ-NPs were dispersed in normal saline at the concentration of 1 mg/mL by mild shaking. The particle size was expressed as intensity-weighed mean diameter in nanometers and obtained from the measurements of at least three batches of ITZ-NPs.

The zeta potential of the ITZ-NPs was measured by NicompTM 380ZLS zeta potential/particle sizer. The preparation of sample was identical to the particle size measurement and the electric field applied was 5 V.

2.3.2. Transmission electron microscopy (TEM) observation

The ITZ-NPs were dispersed into water at a concentration of 5 mg/mL by mild shaking. A drop of ITZ-NPs colloids solution was placed on a TEM copper grid coated with carbon film and dried at room temperature. Morphological observation was performed using a Hitachi H-600 transmission electron microscope (Japan) at 80 kV.

2.3.3. X-ray powder diffractogram (XRD) measurement

To determine the existing form of itraconazole in the ITZ-NPs, XRD measurement was carried out with D/Max-γB diffractometer (Japan) using Ni filtered Cu Kα1 radiation, an accelerating voltage of 40 kV, a beam current of 30 mA, a step size of 0.02°, and a data acquisition time of 2.0 s per step. All experiments were performed at room temperature. The conditions of powder XRD measurement was conducted with a scanning speed of 4°/min between 5 and 40 2θ angle.

2.3.4. Differential scanning calorimetry (DSC)

Accurately weighted samples (5 mg) were placed in nonhermetically sealed aluminum pans. An empty aluminum pan served as a reference. The DSC measurement was done via Differential scanning calorimeters (DSC 204 Phoenix, Germany). The heating rate was 10 K/min and nitrogen purges at a speed of 20 mL/min.

2.3.5. Fourier transform infrared spectroscopy (FT-IR) study

FT-IR spectra were measured using FT-IR spectrophotometer (Thermo Nicolet Avatar 360 FTIR Spectrometer). About 10 mg of sample was mixed with 200 mg of KBr and compressed into a pellet using a hydraulic press. FT-IR spectra over the scanning range of 400–4000 cm^{-1} were obtained with the resolution of 2 cm^{-1}.

2.3.6. Determination of drug incorporation efficiency

1 mg of ITZ-NPs was dissolved in 20 mL of acetonitrile and sonicated for 30 min to extract drug completely. Itraconazole in the solution was measured by high-performance liquid chromatography (HPLC) (LC-10A, Shimadzu, Japan) equipped with a Diamond C18 column (4.6 mm × 250 mm, 5 μm). The mobile phase of 55% acetonitrile and 45% 0.02 M phosphate buffer (pH 3.0) was run isocratically at 25 °C at a flow rate of 1 mL/min, and itraconazole was detected by UV detector at 263 nm. Drug incorporation efficiency was expressed as drug encapsulation efficiency (%, w/w) and drug

content (%, w/w), represented by Eqs. (1) and (2), respectively.

$$\text{Drug encapsulation efficiency (\%)} = \left[\frac{\text{drug remained in the nanoparticles}}{\text{feeding weight of drug}}\right] \times 100 \quad (1)$$

$$\text{Drug content (\%)} = \left[\frac{\text{drug weight in nanoparticles}}{\text{total weight of nanoparticles}}\right] \times 100 \quad (2)$$

2.3.7. Stability test

For dilution stability test, ITZ-NPs and ITZ-CD were diluted in saline at different concentrations and stored at 25 °C for 24 h. The amount of itraconazole remaining in solution was assayed using HPLC.

For the storage stability, ITZ-NPs powder prepared as described above were stored at 4 °C for 6 months. Then the ITZ-NPs were reconstituted in saline by mild shaking, the particle size, zeta potential and drug content of which were determined.

2.3.8. Drug release study

In vitro release of itraconazole from ITZ-NPs was performed as follows: 1 mL of 1 mg/mL ITZ-NPs was sealed in a dialysis bag and immersed in 49 mL PBS containing 10% (v/v) fetal bovine serum (FBS) at 37 °C (Cheung et al., 2004) with a shaking rate of 100 rpm. Sample (0.5 mL each) was withdrawn from the medium at designated time intervals and same volume of fresh medium was added. Each sample was mixed with 1.5 mL of acetonitrile, vortexed for 3 min and centrifuged and the supernatant was assayed by HPLC.

2.4. Safety test of ITZ-NPs

2.4.1. Hemolytic assay

ITZ-NPs and ITZ-CD were respectively diluted into different concentrations between 1.0 and 10.0 mg/mL in saline. To 1.45 mL of each solution, 50 μL of rat blood was added. Following incubation at 37 °C for 60 min, the samples were centrifuged at 5000 rpm for 10 min and the amount of cell lysis or released hemoglobin was measured spectrophotometrically at a wavelength of 540 nm (UV 2401, Shimadzu, Japan).

2.4.2. Acute dose toxicity study

Five male (20–25 g) and five female (20–25 g) mice per dosing group were used. ITZ-CD (10, 20, 40, 80 mg/kg) and ITZ-NPs (10, 20, 40, 80, 160, 320 mg/kg) were administered intravenously through the caudal vein of the mice. An equivalent number of control mice were given saline. Dose related toxicities were observed immediately, 1 h postinjection and then daily for 7 days. The clinical signs, mortality, changes of body weight and the necropsy findings of dead and surviving mice were all examined.

2.5. Pharmacokinetics and tissue distribution study of ITZ-NPs

2.5.1. Animals test

120 mice (20 ± 2 g) were divided into six groups randomly and fasted overnight. A certain amount of ITZ-CD and ITZ-NPs were respectively dispersed in saline to get a final dose of itraconazole of 400 μg/200 μL, which was equivalent to 20 mg/kg. ITZ-CD and ITZ-NPs were administered intravenously via the caudal vein. At each postinjection time interval (t = 2 min, 0.25, 0.5, 1, 2, 4, 8, 12, 24, 36 h), blood was collected, centrifuged to separate plasma (n = 6, per time interval) which was stored at −70 °C. Then the mice (n = 6, per time interval) were sacrificed and the tissues (heart, lung, spleen, liver, kidney and brain) were collected for analysis. All the tissues were blotted with lint-free paper toweling to remove residual blood and stored at −70 °C until analysis.

2.5.2. Analysis of itraconazole and OH-itraconazole in plasma and tissue samples

For the plasma samples, briefly, 100 μL of plasma was pipetted into a 3-mL Eppendorf centrifuge tube, to which 20 μL of internal standard (2 μg/mL), 20 μL of 1 M potassium carbonate solution and 3 mL *tert*-butyl methyl ether was added and vortexed for 2 min. The organic phase was separated and evaporated. Then the residue was reconstituted with 200 μL mobile phase and centrifuged before analysis by RP-HPLC (Wong et al., 2003). For the tissues samples, 300 μL homogenized tissue was taken for analysis and processed similarly to plasma samples.

The analysis was performed on a RP-HPLC (LC-10A, Shimadzu, Japan) with Diamond C18 column (250 mm × 4.6 mm, 5 μm) attached to a C18 guard column (7.5 mm × 4.6 mm, 5 μm, Diamond). The mobile phase of 45% 0.02 M potassium phosphate (pH 3.0) and 55% acetonitrile was run isocratically at 25 °C at a flow rate of 1.0 mL/min. The injection volume was 100 μL. Itraconazole and OH-itraconazole were detected by UV detector at 263 nm.

2.5.3. Pharmacokinetics and statistical analysis

Following analysis described above, pharmacokinetics parameters for itraconazole and OH-itraconazole were derived from mean plasma concentration–time curves and determined using noncompartmental methods with WinNonlin 4.0.1 (Pharsight Corp., CA). The following pharmacokinetic parameters were determined: the peak concentration in plasma (C_{max}), the time to reach maximum concentration (T_{max}), the area under the plasma concentration–time curve (AUC), and elimination half-life ($T_{1/2}$).

Statistical significance of differences was tested using the two-tail Student's t-test. A p-value below 0.05 was considered significant.

3. Results

3.1. Preparation of ITZ-NPs

ITZ-NPs were prepared by nanoparticle albumin bound technology. HSA was important in the process to avoid coalescence and agglomeration during homogenization, which also acted as cryoprotectant and an aid for reconstitution. ITZ-NPs were prepared at different concentrations of HSA (0.5, 1, 2, 3 and 4%). When the HSA concentration was 0.5%, there was not enough HSA to stabilize the interface and the nanoparticles were not stable during reconstitution. At the concentration of 3 and 4%, a great deal of foam was formed during homogenization, which affected the reproducibility of the method. When the concentration of HSA was 1 or 2%, the mean particle sizes of ITZ-NPs were 118.1 ± 1.2 and 108.6 ± 1.6 nm, respectively. So the concentration of HSA in the research was selected as 2%. The influence of drug concentration and ratio of organic solvent and water (v/v) were shown in Table 1. When the drug concentration increased, the mean particle size and drug content of ITZ-NPs scaled up; while when the ratio of organic solvent and water decreased, both the particle size and drug content of ITZ-NPs decreased. To obtain nanoparticles with mean particle size smaller than 120 nm and with satisfied drug encapsulation and drug content, HSA concentration was selected as 2% (w/w), the drug concentration was 50 mg/mL and the ratio of organic phase/water was 1:19 in this experiment.

For four batches of ITZ-NPs, the mean particle size was found to be 108.6 ± 1.6 nm. The polydispersity index was 0.099 ± 0.002. The zeta potential of nanoparticles was −25.1 ± 0.6 mV. Drug encapsu-

Table 1
Characteristics of the nanoparticles involved in ITZ-NPs preparation studies ($n = 3$)

HSA concentration (%, w/w)	Drug concentration (mg/mL)	Organic phase:water (v/v)	Mean particle size (nm)	Zeta potential ± S.D. (mV)	Drug content ± S.D. (%)	Drug entrapment (%)
2	25	1:19	80.5 ± 2.1	−24.2 ± 0.8	5.5 ± 0.2	89.7 ± 0.2
2	50	1:19	108.6 ± 1.6	−25.1 ± 0.6	11.1 ± 0.5	95.1 ± 0.5
2	75	1:19	125.3 ± 2.8	−25.9 ± 0.7	14.2 ± 1.1	86.0 ± 0.3
2	50	1:9	129.5 ± 3.7	−23.4 ± 1.3	17.1 ± 1.6	78.7 ± 0.6
2	50	1:29	119.8 ± 1.9	−23.6 ± 2.1	7.2 ± 0.7	90.2 ± 0.4
2	50	1:49	107.2 ± 2.8	−24.8 ± 1.5	4.4 ± 0.5	91.1 ± 0.3
2	50	1:74	101.0 ± 3.2	−24.1 ± 2.0	3.2 ± 0.2	96.4 ± 0.9

lation efficiency was 95.1 ± 0.5%, and the drug loading content was 11.1 ± 0.5%.

In reconstitution stability test, the drug content of both ITZ-NPs and ITZ-CD showed no difference when the concentration of itraconazole was 10, 5, 3.3 mg/mL, respectively. However, when the concentration of itraconazole was below 2 mg/mL, itraconazole in the solution of ITZ-CD would precipitate from the solution, and the drug remaining in the solution was only 86.9 ± 1.6%, while that of ITZ-NPs was 98.9 ± 0.7% and no precipitation appeared. So, it was concluded that the ITZ-CD was unstable when the itraconazole concentration was less than 3.33 mg/mL, while ITZ-NPs were stable at a wide range of concentrations at 25 °C for 24 h. The phenomenon of precipitation was identical to prior report (Yi et al., 2007). As for the precipitation formation of ITZ-CD, ITZ-CD was suggested to be A_P-type solubility relationships, indicating higher order complexation at higher HP-β-CD concentration (Peeters et al., 2002). Precipitation may occur in such systems at any dilution where the equilibrium drug solubility is lower than the dilution concentration line at a given cyclodextrin concentration (Rajewski and Stella, 1996). Hence, it is critical for ITZ-CD to maintain a 3.33 mg/mL itraconazole (Thomson and Montvale, 2005).

After stored at 4 °C over 6 months, the mean particle size and S.D. of the ITZ-NPs was 108.8 ± 1.82 nm, polydispersity index was 0.098 ± 0.002, and the drug content remained 11.1 ± 0.1%. The results indicated that ITZ-NPs were stable at 4 °C for 6 months.

3.2. Physicochemical characterization of ITZ-NPs

Transmission electron microscopy (TEM) was utilized to evaluate the morphology of the ITZ-NPs. As shown in Fig. 1, the particles showed spherical shapes with particle size about 100 nm.

X-ray powder diffraction was used to determine the crystalline or non-crystalline nature of itraconazole in the lyophilized nanoparticles powder. As shown in Fig. 2, itraconazole powder showed strong typical peaks of crystalline itraconazole; lyophilized HSA showed broad typical humps of amorphous material of HSA; a physical mixture of itraconazole and albumin showed the broad humps of HSA, while the peak of itraconazole was also apparently visible; the itraconazole nanoparticles lyophilized powder showed no evidence of crystalline characteristics of itraconazole and appeared identical to that of HSA, indicating that itraconazole was at an amorphous state in the ITZ-NPs.

DSC was also utilized to investigate the existing form of itraconazole in ITZ-NPs. As shown in Fig. 3, the melting endothermal peak of bulk itraconazole was recorded at 167.1 °C, while that of lyophilized albumin was recorded at 146.7 and 214 °C. The physical mixture of itraconazole and HSA showed both features of them. However, the ITZ-NPs showed only HSA endothermal peaks but no peak of itraconazole. It could be concluded that itraconazole did not exist in the ITZ-NPs as crystal and had mutual effect with HSA.

The ITZ-NPs in both DSC and X-ray powder diffraction test had been stored for 1 month at 4 °C prior to analysis and no crystal was observed during storage of the lyophilized products.

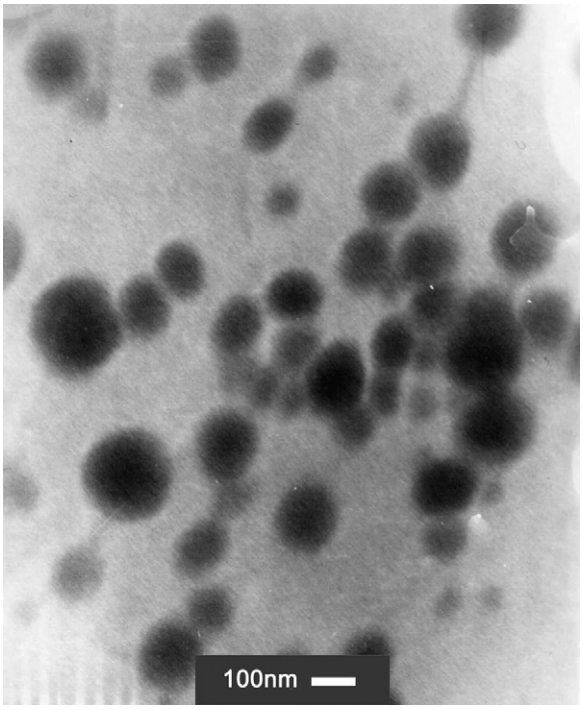

Fig. 1. TEM photographs of ITZ-NPs. Electron microscopy (magnification: 100,000×), the concentration of ITZ-NPs solution was 5 mg/mL.

FT-IR analysis was made to detect the interactions between itraconazole and HSA. As shown in Fig. 4, specific FT-IR spectra of itraconazole powders were noticed at 400–1800 cm^{-1}. The characteristic peaks of itraconazole at 1700, 1520 and 1230 cm^{-1} were observed in the physical mixture of HSA and itraconazole, which could not be observed in spectra of ITZ-NPs. This suggested that there were some interactions between itraconazole and HSA in the ITZ-NPs.

The *in vitro* drug release kinetics of ITZ-NPs was shown in Fig. 5. The cumulative release of itraconazole during the initial 15 min was 24.1 ± 1.2%. The rest of itraconazole in the ITZ-NPs was continuously released over 24 h. The initial burst release could help the drug delivery system quickly reach the therapeutic concentration, which was quite important for antifungal drugs. The burst release was caused by the itraconazole bound with the free HSA in the reconstituted solution or with the HSA at the surface of nanoparticles (Desai et al., 1999).

3.3. Safety

Hemolytic potential of ITZ-NPs was evaluated with rat blood to ensure its hemocompatibility. As shown in Table 2, when the concentrations of itraconazole were 10.0, 5.0, 3.3 and 1.0 mg/mL, the hemolysis of ITZ-NPs was 20.1, 12.1, 3.7 and 2.1% respectively. On

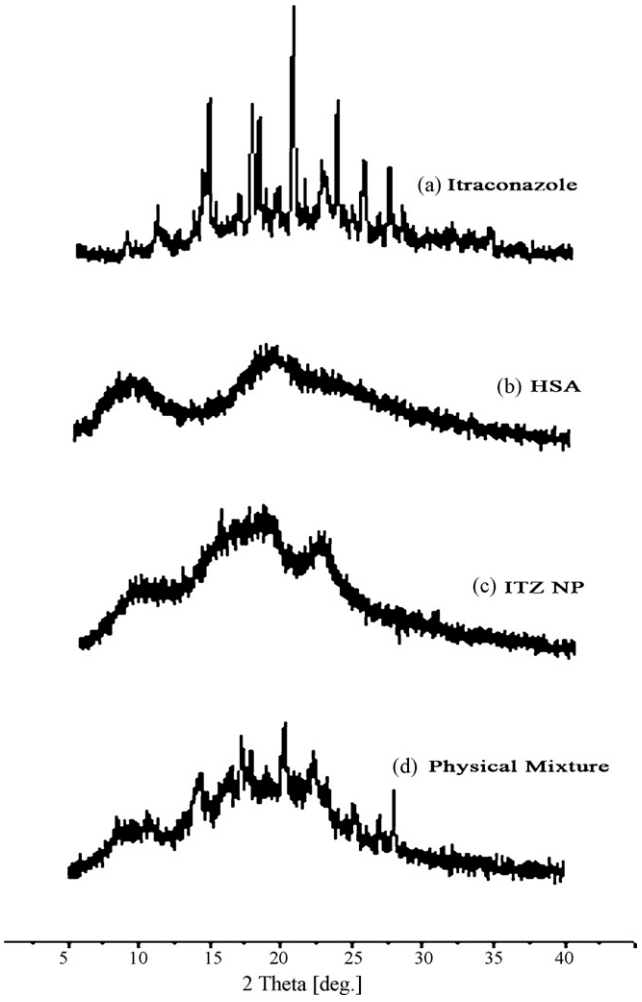

Fig. 2. XRD powder diffractogram of itraconazole (a), human serum albumin (HSA) (b), ITZ-NPs (c) and the physical mixture of human serum albumin/itraconazole (weight ratio of itraconazole/HSA = 1/9) (d).

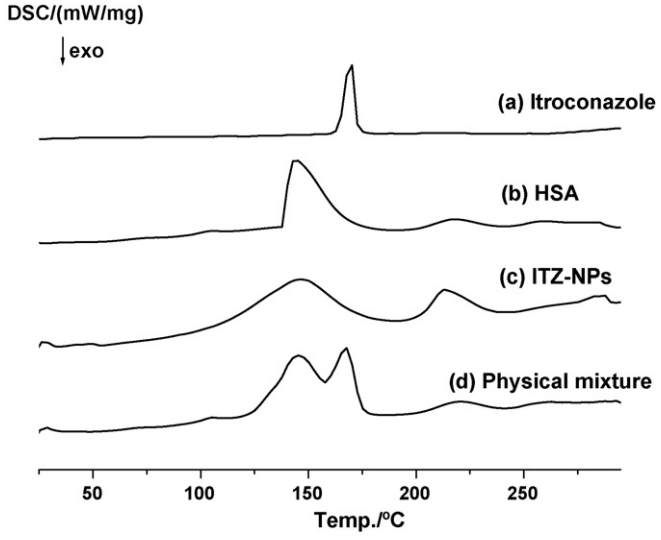

Fig. 3. DSC of itraconazole (a), human serum albumin (HSA) (b), ITZ-NPs (c) and physical mixture of human serum albumin/itraconazole (weight ratio of itraconazole/HSA = 1/9) (d).

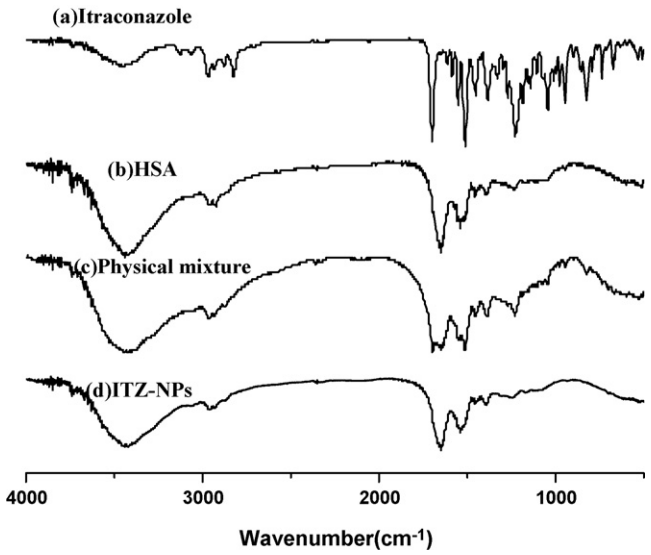

Fig. 4. FT-IR spectra of itraconazole (a), HSA (b), physical mixture of HSA/itraconazole (weight ratio of itraconazole/HSA = 1/9) (c) and ITZ-NPs (d).

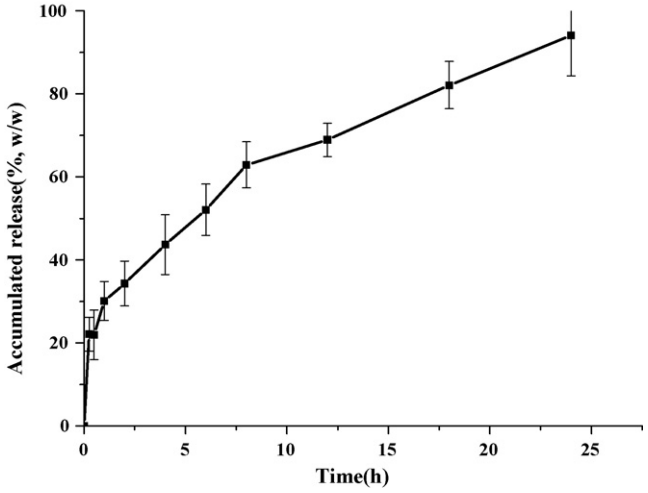

Fig. 5. *In vitro* release curve of ITZ-NPs in 10% fetal bovine serum.

the other hand, ITZ-CD caused much more serious hemolysis. When the concentrations of itraconazole were 10.0, 5.0 and 3.3 mg/mL, the hemolysis was 94.9, 83.2 and 66.4%, respectively. When it was further diluted to be 1.0 mg/mL, itraconazole precipitated from the solution. The results indicated that ITZ-NPs were more biocompatible than ITZ-CD because of milder hemolysis.

The acute toxicity of ITZ-NPs was investigated after intravenous (i.v.) bolus injection to mice. Two of 10 mice treated with 320 mg/kg ITZ-NPs showed hypoactivity immediately and the signs disap-

Table 2
Hemolytic potential of ITZ-NPs and ITZ-CD after incubation at 37 °C for 1 h in rat blood ($n = 3$)

Concentration (mg/mL)	Hemolysis (%)	
	ITZ-CD	ITZ-NPs
10.0	94.9 ± 5.3	20.1 ± 2.7
5.0	83.2 ± 3.3	12.1 ± 2.9
3.3	66.4 ± 6.9	3.7 ± 1.9
1.0	N.D.	2.1 ± 1.2

N.D.: not determined due to drug precipitation.

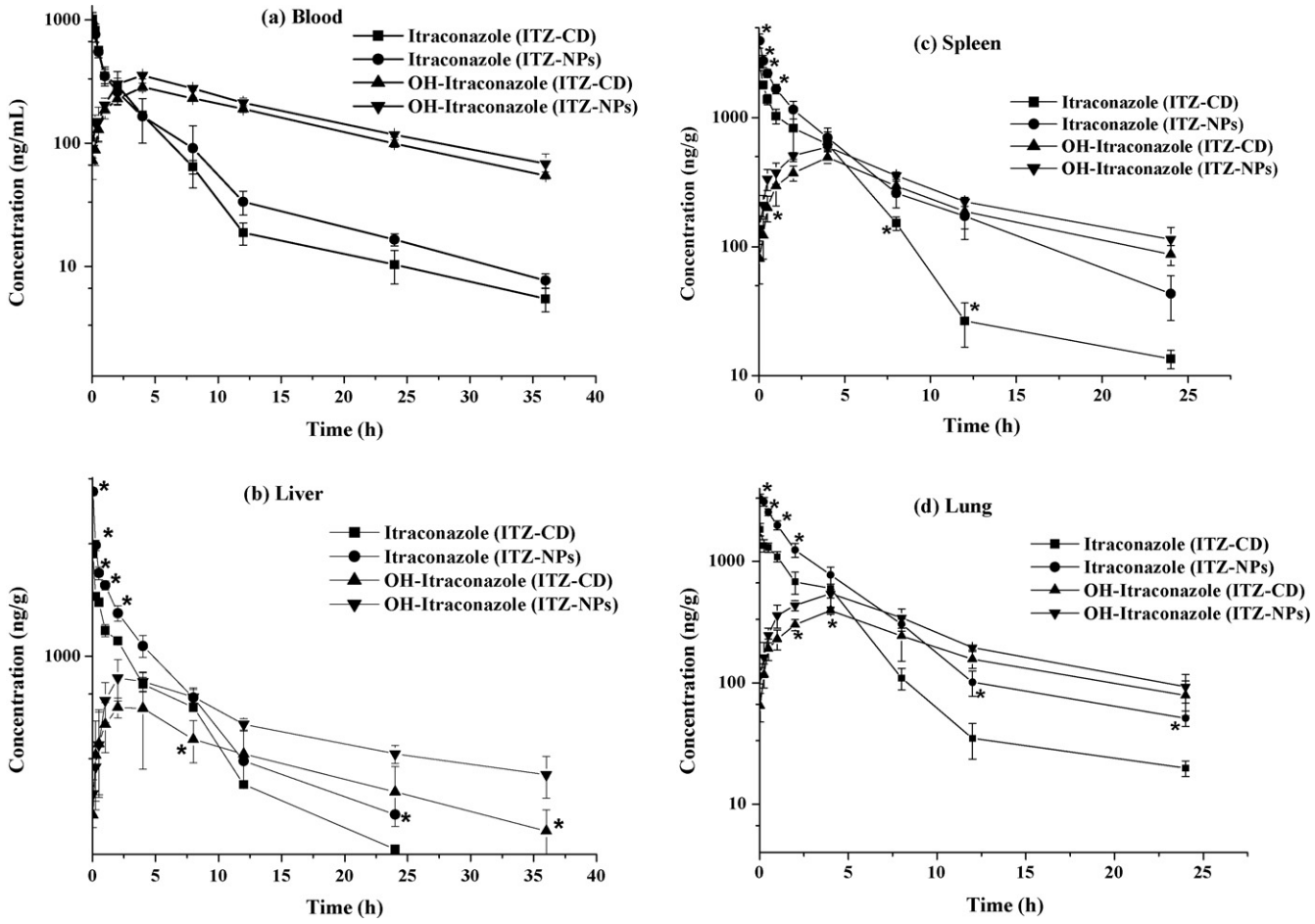

Fig. 6. Concentration–time profiles of itraconazole and OH-itraconazole in blood (a), liver (b), spleen (c) and lung (d) after single i.v. administration to mice at a dose of 20 mg/kg. Each point represents mean ± S.D. ($n = 6$). The asterisks indicate a statistically significant difference between ITZ-CD and ITZ-NPs treatments ($p < 0.05$).

peared in 1 h. No symptoms were observed in ITZ-NPs groups (20, 40, 80 and 160 mg/kg) and ITZ-CD groups (20 and 10 mg/kg). Six of 10 mice treated with 80 mg/kg of ITZ-CD died within a few minutes postdosing. No mortality was observed at the dose of 40 mg/kg of ITZ-CD. Yet, 3 of 10 mice showed hypoactivity and irregular breathing immediately after injection and the signs disappeared within 1 h. No group difference appeared for body weight gain over the 7-day duration of the study for saline group, ITZ-CD groups (10, 20 and 40 mg/kg) and ITZ-NPs groups (20, 40, 80 and 160 mg/kg). At necropsy, no macroscopic abnormalities were observed in all mice. For ITZ-NPs, the no-observed-effect level (NOEL) was 160 mg/kg; and for ITZ-CD was 20 mg/kg. NOEL is defined as the highest dose that had no effect on any of the measurement parameters in any of the studies (Rabinow et al., 2007). Thus, it was concluded that ITZ-NPs showed better tolerance in mice than ITZ-CD did.

3.4. Pharmacokinetics and tissue distribution

After i.v. bolus injections of ITZ-NPs and ITZ-CD to mice (20 mg/kg), the average plasma concentration vs. time curves of itraconazole and OH-itraconazole were determined (Fig. 6a). Itraconazole showed a rapid distribution phase of less than 1 h and its terminal elimination half-life was 4–6 h. OH-itraconazole was detected from the first blood sampling time (2 min) and reached its C_{max} at 4 h. The pharmacokinetic parameters were listed in Table 3, and there were no differences of the pharmacokinetic parameters of itraconazole and OH-itraconazole between the two formulations.

In tissue distribution study, more itraconazole and OH-itraconazole were detected in tissues than in plasma. For both itraconazole and OH-itraconazole, there were no differences of distributions in the heart, kidney and brain between two formulations, and at most indicated time the OH-itraconazole levels in the liver, spleen and lung had no differences between two formulations, either. Nevertheless, in the liver, spleen and lung, itraconazole levels for the group treated with ITZ-NPs were significantly higher than those for the group treated with ITZ-CD. The average tissue concentration in liver, spleen and lung vs. time curves were shown in Fig. 6b–d. For the group treated with ITZ-NPs, the ratios of AUC of itraconazole between the three tissues (liver, spleen and lung) and plasma were 6.32, 3.86 and 4.00, respectively. For the group treated with ITZ-CD, the ratios of AUC of itraconazole between the tissues and plasma were 4.99, 2.63 and 2.38, respectively. In the liver, the AUC of itraconazole for the ITZ-NPs group was 1.4-fold higher than that of ITZ-CD group, in the spleen was 1.6-fold and in the lung was 1.83-fold. As for the higher distribution in the spleen and liver of ITZ-NPs, a murine reticuloendothelial system (RES) might be involved (Grislain et al., 1983; Yamashita et al., 1991; Li et al., 2008).

4. Discussion

In the past 5 years, self-emulsion drug delivery system (Hong et al., 2006), nanosuspension (Matteucci et al., 2006; Rabinow et al., 2007), biodegradable nanoparticles (Prakobvaitayakit and Nimmannit, 2003) and polymer micelles (Yi et al., 2007) have

Table 3
Comparison of pharmacokinetic parameters after single i.v. administration ITZ-NPs and ITZ-CD to mice at a dose of 20 mg/kg ($n = 6$)

Analyte	Treatment	C_{max} (ng/mL)	T_{max} (h)	AUC_{36h} (μg h/mL)	$T_{1/2}$ (h)
Itraconazole	ITZ-NPs	929.87 ± 88.9	0.03	2546.56	5.80
	ITZ-CD	1051.12 ± 130.5	0.03	2327.12	4.20
Hydroxy-itraconazole	ITZ-NPs	354.31 ± 21.5	4.00	6407.01	9.06
	ITZ-CD	284.77 ± 21.8	4.00	5381.65	9.00

been utilized to overcome the insolubility of itraconazole. Polymers, oil or surfactants were used in these technologies to stabilize the itraconazole. Although these non-endogenous materials are biodegradable, they could cause problems of slow clearance, immunogenicity when administered intravenously. HSA is much superior to these materials as a hydrophilic endogenous protein.

Albumin nanoparticles could be prepared by desolvation or emulsification followed by denaturation through heating or chemical crosslinking (Weber et al., 2000; Wartlick et al., 2004; Dreis et al., 2007). However, these methods were not suitable for water-insoluble drugs, and the final state of albumin was different from that in nanoparticle albumin bound technology. In the condition of chemical crosslinking process, amines or hydroxyls present in the HSA were cross-linked nonspecifically and essentially. And the structure of HSA in the heat denaturation was also irreversibly altered. In contrast, the ITZ-NPs preparation, the sulfhydryl residues of the HSA may be oxidized (and/or disrupting existing disulfide bonds) to form new, crosslinking disulfide bonds, as a result of the tremendous local heating from the cavitation in the liquid by the high-pressure homogenizer. But the disulfide formation contemplated by the homogenization did not substantially denature the HSA (Desai et al., 1999). On the other hand, no other surfactants, polymer or toxic solvents were involved in the final product of ITZ-NPs. Hence, the ITZ-NPs were safe and biocompatible for intravenous usage and the conclusion were approved by two facts in present work. Firstly, when the concentration of itraconazole was 10 mg/mL, ITZ-NPs caused mild hemolysis while the hemolysis of ITZ-CD was fivefold higher. Secondly, the tolerance of ITZ-NPs was notably better than ITZ-CD in mice.

The pharmacokinetic parameters of itraconazole or OH-itraconazole showed no differences between ITZ-NPs and ITZ-CD, indicating that the substitution of HSA for HP-β-CD had no influence on the pharmacokinetics of itraconazole and OH-itraconazole.

Nanoparticulate drug carriers after intravenous administration would be uptaken by the RES (Gref et al., 1994). Like other nanoscale drug delivery systems, the distributions of itraconazole for ITZ-NPs in liver and spleen were significantly higher than those of ITZ-CD at most indicated time. It has been reported that particle size and surface character of nanoparticles were two key factors influencing the uptake amount of nanoparticles by RES, The smaller the particle size was or the more hydrophilic the surface was, the longer the nanoparticles stayed in the plasma (Ogawara et al., 1999; Esmaelli et al., 2008). In present work, the mean particle size of ITZ-NPs was about 100 nm. Meanwhile, the HSA at the surface of the ITZ-NPs improved the hydrophilicity of the ITZ-NPs. And it has been reported that albumin might provide dysopsonin-like activity by inhibiting the subsequent association of opsonins on the surface of nanospheres (Ogawara et al., 1999) and liposomes (Furumoto et al., 2007). Hence, the nanoscale particle size and the hydrophilic HSA on the ITZ-NPs' surface might decrease the uptake of nanoparticles by RES. And it was supposed that the ITZ-NPs would cause less hepatic toxicity than nanoparticles prepared with other hydrophobic materials.

Nevertheless, the higher distribution of itraconazole in lung for ITZ-NPs had not been reported in other nanoparticles study, maybe it was related to the utilization of HSA. It was worth noticing because in immunocompromised patients the portal of entry was typically the lungs where the fungi would present as pneumonia, cavitary infiltrates or nodules (Singh and Husain, 2003). Hence, the ITZ-NPs showed a potential in treating fungi infected lung diseases.

5. Conclusion

Itraconazole-loaded nanoparticles (ITZ-NPs) were prepared based on HSA via nanoparticle albumin bound technology. The product could be sterile-filtered and provide stable solution at a wide range of concentrations. The DSC, X-ray powder diffraction and FT-IR measurement revealed that itraconazole did not exist in the ITZ-NPs as crystal and had mutual effect with HSA. Hemolysis assay and acute dose toxicity study revealed that ITZ-NPs were more biocompatible than the cyclodextrin formulation of itraconazole (ITZ-CD) because of the substitution of HSA for HP-β-CD. The pharmacokinetic parameters after intravenous administration to mice showed no difference from those of ITZ-CD, indicating that the use of HSA in the ITZ-NPs formulation had no influence on the pharmacokinetic properties of itraconazole and OH-itraconazole. In comparison with the ITZ-CD, tissue distribution study revealed higher level of itraconazole and OH-itraconazole in liver, spleen and lung in ITZ-NPs treated group. Meanwhile, the high distribution of ITZ-NPs in lung was of great potential to the therapy of pneumonia infection. The results indicate that the ITZ-NPs appear to be a promising intravenous formulation of itraconazole.

Acknowledgements

This work was supported by the National Basic Research Program of China (973 Program) (no. 2007CB935800) and Shanghai key Technologies R&D Program (no. 074319117).

References

Cheung, R.Y., Kuba, R., Rauth, A.M., Wu, X.Y., 2004. A new approach to the in vivo and in vitro investigation of drug release from locoregionally delivered microspheres. J. Control. Release 100, 121–133.
Cohen, B.E., 1998. Amphotericin B toxicity and lethality: a tale of two channels. Int. J. Pharm. 162, 95–106.
Desai, N.P., Tao, C., Yang, A., Louie, L., Zheng, T.L., et al., 1999. Protein stabilized pharmacologically active agents, methods for the preparation thereof and methods for the use thereof. U.S. Patent No. 5,916,596.
Dreis, S., Rothweiler, F., Michaelis, M., Cinatl Jr., J., Kreuter, J., Langer, K., 2007. Preparation, characterization and maintenance of drug efficacy of doxorubicin-loaded human serum albumin (HSA) nanoparticles. Int. J. Pharm. 341, 207–214.
Edwards, J.E., Bodey, G.P., Bowden, R.A., Büchner, T., de Pauw, B.E., Filler, S.G., Ghannoum, M.A., Glauser, M., Herbrecht, R., Kaufmann, C.A., Kohno, S., Martino, P., Meunier, F., Mori, T., Pfaller, M.A., Rex, J.H., Rogers, T.R., Rubin, R.H., Solomkin, J.C., Viscoli, C., Walsh, T.J., White, M., 1997. International conference for the development of a consensus on the management and prevention of severe candidal infections. Clin. Infect. Dis. 25, 43–59.
Esmaelli, F., Ghahremani, M.H., Esmaeili, B., Esmaeili, B., Khoshayand, M.R., Atyabi, F., Dinarvand, R., 2008. PLGA nanoparticles of different surface properties: preparation and evaluation of their body distribution. Int. J. Pharm. 349, 249–255.
Furumoto, K., Yokoe, J., Ogawara, K., Amano, S., Takaguchi, M., Higaki, K., Kai, T., Kimura, T., 2007. Effect of coupling of albumin onto surface of PEG liposome on its in vivo disposition. Int. J. Pharm. 329, 110–116.
Grant, S., Clissold, S., 1989. Itraconazole: a review of its pharmacodynamic and pharmacokinetic properties and therapeutic use in superficial and systemic mycoses. Drug 37, 310–344.

Gref, R., Minamitake, Y., Peracchia, M.T., Tubetskoy, V., Torchilin, V., Langer, R., 1994. Biodegradable long-circulating polymeric nanospheres. Science 263, 1600–1603.
Grislain, L., Couvreur, P., Lenaerts, V., Roland, M., Deprez-Decampeneere, D., Speiser, P., 1983. Pharmacokinetics and distribution of a biodegradable drug-carrier. Int. J. Pharm. 15, 335–345.
Groll, A.H., Wood, L., Roden, M., Mickiene, D., Chiou, C.C., Townley, E., Dad, L., Piscitelli, S.C., Walsh, T.J., 2002. Safety, pharmacokinetics and pharmacodynamics of cyclodextrin itraconazole in pediatric patients with oropharyngeal candidiasis. Antimicrob. Agents Chemother. 46, 2554–2563.
Heykants, J., Michiels, M., Meuldermans, W., Monbaliu, J., Lavrijsen, K., Van Peer, A., Levron, J.C., Woestenborghs, R., Cauwenbergh, G., 1987. The pharmacokinetics of itraconazole in animals and man: an overview. In: Fromtling, R.A. (Ed.), Recent Trends in the Discovery, Development and Evaluation of Antifungal Agents. J.R. Prous Science Publishers, Barcelona, Spain, pp. 57–83.
Hong, J.Y., Kim, J.K., Song, Y.K., Park, J.S., Kim, C.K., 2006. A new self-emulsifying formulation of itraconazole with improved dissolution and oral absorption. J. Control. Release 110, 332–338.
Li, F.Q., Su, H., Wang, J., Liu, J.Y., Zhu, Q.G., Fei, Y.B., Pan, Y.H., Hu, J.H., 2008. Preparation and characterization of sodium ferulate entrapped bovine serum albumin nanoparticles for liver targeting. Int. J. Pharm. 349, 274–282.
Lortholary, O., Denning, D.W., Dupont, B., 1999. Endemic mycoses: a treatment update. J. Antimicrob. Chemother. 43, 321–331.
Matteucci, M.E., Hotze, M.A., Johunston, K.P., Williams, R.O., 2006. Drug nanoparticles by antisolvent precipitation: mixing energy versus surfactant stabilization. Langmuir 22, 8951–8959.
Mikami, Y., Sakamoto, T., Yazawa, K., Gonoi, T., Ueno, Y., Hasegawa, S., 1994. Discrepancies in bioassay and chromatography determinations explained by metabolism of itraconazole to hydroxyitraconazole: studies of interpatient variations in concentrations. Antimicrob. Agents Chemother. 37, 2224–2227.
Odds, F.C., Bossche, H.V., 2000. Antifungal activity of itraconazole compared with hydroxy-itraconazole in vitro. J. Antimicrob. Chemother. 45, 371–373.
Ogawara, K., Yoshida, M., Higaki, K., Kimura, T., Shiraishi, K., Nishikawa, M., Takakura, Y., Hashida, M., 1999. Hepatic uptake of polystyrene microspheres in rats: effect of particle size on intrahepatic distribution. J. Control. Release 59, 15–22.
Peeters, J., Neeskens, P., Tollenaere, J.P., Van, P., Brewster, M., 2002. Characterization of the interaction of 2-hydroxy-β-cyclodextrin with itraconazole at pH 2, 4 and 7. J. Pharm. Sci. 91, 1414–1422.
Phillips, P., De Beule, K., Frechette, G., Tchamouroff, S., Vandercam, B., Weitner, L., Hoepelman, A., Stingl, G., Clotet, B., 1998. A double-blind comparison of itraconazole oral solution and fluconazole capsules for the treatment of oropharyngeal candidiasis in patients with AIDS. Clin. Infect. Dis. 26, 1368–1373.
Picardi, M., Camera, A., Luciano, L., Ciancia, R., Rotoli, B., 2003. Intravenous itraconazole for treating invasive pulmonary aspergillosis in neutropenic patients with acute lymphoblastic leukemia. Haematologica 88, ELT01.
Prakobvaitayakit, M., Nimmannit, U., 2003. Optimization of polylactic-co-glycolic acid nanoparticles containing itraconazole using 2^3 factorial design. AAPS PharmSciTech. 4, 565–573.
Rabinow, B., Kipp, J., Papadopoulos, P., Wong, J., Glosson, J., Gass, J., Sun, C.S., Wielgos, T., White, R., Cook, C., Barker, K., Wood, K., 2007. Itraconazole IV nanosuspension enhances efficacy through altered pharmacokinetics in the rat. Int. J. Pharm. 339, 251–260.
Rajewski, R.A., Stella, V.J., 1996. Pharmaceutical applications of cyclodextrins. 2. *in vivo* drug delivery. J. Pharm. Sci. 85, 1142–1169.
Revankar, S., Kirkpatrick, W., McAtee, R., Dib, O., Fothergill, A., Redding, S., Rinaldi, M., Patterson, T., 1996. Detection and significance of fluconazole resistance in orpharyngeal candidiasis in human immunodeficiency virus infected patients. J. Infect. Dis. 174, 821–827.
Rex, J., Pfaller, M., Galgiani, J., Bartlett, M., Espinel-Ingroff, A., Ghannoum, M., Lancaster, M., Odds, F., Rinaldi, M., Walsh, T., Barry, A., 1997. Development of interpretive breakpoints for antifungal susceptibility testing: conceptual framework and analysis of in vitro–in vivo correlation data for fluconazole, itraconazole, and *Candida infections*. Clin. Infect. Dis. 24, 235–247.
Sheehan, D.J., Hitchcock, C.A., Sibley, C.M., 1999. Current and emerging azole antifungal agents. Clin. Microbiol. Rev. 12, 40–79.
Singh, N., Husain, S., 2003. Aspergillus infections after lung transplantation: clinical differences in type of transplant and implications for management. J. Heart Lung Transplant. 22, 258–266.
Thomson, P.D.R., Montvale, N.J., 2005. Physician's Desk Reference, 59th, pp. 1757–1766.
Van Cauteren, H., Heykants, J., De Coster, R., Cauwenbergh, G., 1987. Itraconazole: pharmacologic studies in animals and humans. Rev. Infect. Dis. 9, S43–S46.
Walsh, T.J., Teppler, H., Donowitz, G.R., Maertens, J.A., Baden, L.R., Dmoszynska, A., Cornely, O.A., Bourque, M.R., Lupinacci, R.J., Sable, C.A., dePauw, B.E., 2004. Caspofungin versus liposomal amphotericin B for empirical antifungal therapy in patients with persistent fever and neiutropenia. N. Engl. J. Med. 351, 1391–1402.
Wartlick, H., Spänkuch-Schmitt, B., Strebhardt, K., Kreuter, J., Langer, K., 2004. Tumour cell delivery of antisense oligonuclceotides by human serum albumin nanoparticles. J. Control. Release 96, 483–495.
Weber, C., Kreuter, J., Langer, K., 2000. Desolvation process and surface characteristics of HSA-nanoparticles. Int. J. Pharm. 196, 197–200.
Wong, J.W., Nisar, U.R., Yuen, K.H., 2003. Liquid chromatographic method for the determination of plasma itraconazole and its hydroxyl metabolite in pharmacokinetic/bioavailability studies. J. Chromatogr. B 798, 335–360.
Yamashita, C., Matsuo, H., Akiyama, K., Kiwada, H., 1991. Enhancing effect of cetylmannoside on targeting of liposomes to Kupffer cells in rats. Int. J. Pharm. 70, 225–233.
Yi, Y., Yoon, H.J., Kim, B.O., Shim, M., Kim, S.O., Hwang, S.J., Seo, M.H., 2007. A mixed polymeric micellar formulation of itraconazole: characteristics, toxicity and pharmacokinetics. J. Control. Release 117, 59–67.